JOURNAL OF MATERIALS SCIENCE 28 (1993) 3291–3297

Structural analysis and catalytic activity of sol–gel–prepared Zn–Cr–O

L. FORNI*, C. OLIVA, F. P. VATTI
Dipartimento di Chimica Fisica ed Elettrochimica, Universitá di Milano, via C. Golgi 19, 20133 Milano, Italy

V. Y. TUGARINOV, A. V. VISHNIAKOV
D. I. Mendeleev Institute of Chemical Technology, Miusskaya Sq. 9, Moscow, Russia

Some Zn–Cr–O–based catalysts for the synthesis of methylpyrazine from ethylenediamine and propylene glycol were prepared through the sol–gel technique, from aqueous nitrates and polyacrylic acid. The oxide mixtures so obtained were analysed by several techniques, including scanning electron microscopy, electron probe microanalysis, X-ray diffraction, electron spin resonance (ESR), sorption–desorption of nitrogen, etc. The catalytic activity was tested by the pulse-reactor technique and with a temperature-programmed desorption–reaction apparatus. All the data were compared with those previously collected on similar catalysts prepared either by the wet-mixing procedure or by coprecipitation. It was found that the structure of the solid depends strongly on the method of preparation, besides the chemical composition. The selectivity to the desired product peaked for Zn/Cr = 3 and the smaller the crystal size of the powder, the better the catalyst was found to perform. The ESR signal generated by the Cr^{3+} ions may constitute a useful tool for monitoring both the intimate structure and the catalytic behaviour of the material.

1. Introduction

In previous papers [1–3] it was reported that a mixture of ZnO and Zn chromite is an effective and selective catalyst for the synthesis of methylpyrazine (MP) from ethylenediamine (ED) and propylene glycol (PG), especially when the overall atomic ratio Zn/Cr approaches 3/1. Furthermore, it was observed that the selectivity of the catalyst is affected by the method of preparation, the coprecipitation under controlled conditions being preferred with respect to the wet-mixing procedure [2]. Another interesting observation was the dependence of the electron spin resonance (ESR) signal generated by the solid on catalyst composition [1]. A mechanistic study of the reaction has been reported in further papers, showing also in detail the polyfunctionality of the catalyst [4, 5].

In the present paper we report on the structural analysis of three Zn–Cr–O catalysts, having a Zn/Cr ratio around 3/1, but prepared by the sol–gel technique. Furthermore, a detailed analysis of the catalytic behaviour of the present samples is also reported, together with a comparison of their most interesting physico-chemical characteristics with those measured on the previous catalysts of the same composition.

2. Experimental procedure

2.1. Materials

All the reagents employed for the preparation of catalysts and as reactants for the activity tests were "pro analysi" pure commercial products from Merck, C. Erba, Fluka or Aldrich and were employed as supplied. The carrier gas for the temperature-programmed desorption–reaction (TPD–TPR) experiments was SIAD UP grade He, $\geq$ 99.99995 vol % pure. It was further purified by passing through a high-temperature Supelco High Capacity gas purifier, followed by a Supelco OMI-1 indicating purifier. The total concentration of water + oxygen in the gas coming from the purification system was found to be lower than 0.05 p.p.m.

2.2. Catalysts

The three Zn–Cr–O mixtures, referred to as A, B and C, were prepared by mixing aqueous solutions of the nitrates in the desired proportions, nominally 2.5/1, 3.0/1 and 3.5/1 as Zn/Cr atomic ratio. The resulting solution was added slowly and under vigorous stirring to a 30 wt % aqueous solution of polyacrylic acid (MW ca. 4000) in ample excess (ca. 3 mol of polyacrylic acid per 1 mol of Zn + Cr). The pH of the resulting highly viscous solutions was ca. 1.5. The mixture was then heated cautiously on electric plate for 0.5 h, with formation of a violet polymeric gel. The gel was calcined in air at 440 °C for 3 h with formation of a grey-greenish powder and simultaneous disappearance of any trace of polyacrylic acid. The samples were finally reduced in a slowly flowing 10% H_2 in He gas mixture for 0.5 h at 320 °C.

*To whom all correspondence should be addressed.

0022–2461

All the samples were analysed by X-ray diffraction (XRD) by means of a Siemens D-500 powder diffractometer, employing CuK_α radiation, Ni-filtered. The morphology and the composition of the catalysts were analysed by scanning electron microscope–electron probe microanalyser (SEM-EPMA) on a Cambridge Stereoscan 150 apparatus. ESR spectra were recorded by means of a Varian E-line Century Series apparatus. BET surface area and porosity were determined by N_2 sorption–desorption on a C. Erba Sorptomatic 1800 instrument.

2.3. Apparatus

Comparison tests were carried out by the pulse reactor technique by means of a temperature-programmed desorption–reaction–mass spectrometric (TPD–TPR–MS) apparatus described in detail elsewhere [6].

2.4. Procedure

Different procedures were followed for the collection of TPD–TPR experimental data, depending on the information desired. Such procedures have been determined in previous work and are described in detail elsewhere [4]. Briefly, in each run a fresh catalyst sample (ca. 90 mg) was charged and activated *in situ*, prior to the run, by reduction in a slowly flowing $H_2/He = 1/9$ gas mixture at 320 °C for 0.5 h. Isothermal runs were always carried out at 390 °C, the optimal reaction temperature determined in previous work [1, 2]. The TPD ramps were carried out in every case at 20 °C min^{-1} from the initial 100 °C isotherm, held for 15 min, up to the final one (500 °C), held for 5 min. The carrier gas flow rate was 20 cm^3 min^{-1}.

The sorptive–desorptive behaviour of the catalyst towards the two reactants was analysed by preadsorbing ED or PG through some pulses during the initial isotherm, followed by the TPD ramp. The competition in adsorption between the two reactants was analysed similarly, through preadsorption of one of them before the other, followed by the TPD ramp. The reactivity of the two reactants was tested under either isothermal (390 °C) or non-isothermal conditions: in the first case, by injecting 5 mm^3 pulses of each reactant or an equimolar mixture of both; in the second case, by injecting pulses of one of the reactants during the TPD ramp following the preadsorption of the other.

Continuous monitoring of the composition of the gas leaving the reactor was made through the quadrupolar mass spectrometer (MS) of the apparatus. Unfortunately, the simultaneous presence of mass fragments of the same a.m.u. value was noticed in the individual spectra of many of our species [4, 5, 7, 8]. Hence a rather lengthy search, based on the contemporary monitoring of several fragments, was needed to characterize correctly at least one typical fragment for each species, not perturbed by the same fragment originating from the other species. This is the reason why in the following every species is monitored through only one typical fragment, usually not corresponding to the most abundant one for that species.

3. Results and discussion

3.1. Surface area and porosity

The BET surface area and the porosity of the present three catalyst samples are shown in Table I.

3.2. SEM–EPMA and XRD analysis

Several attempts were made to dissolve the catalysts by the usual alkaline fusion technique, in order to carry out chemical analysis by the UV–visible spectrophotometric procedure followed previously [1]. Unfortunately, only poorly reproducible results were obtained in the present case, due to the quite difficult disaggregability of the solid. Better results were obtained by determining the Zn/Cr ratio by EPMA [9]. Four standards were prepared by finely and thoroughly grinding in an agate mortar a mixture of pure ZnO and Cr_2O_3 powders in 1/1, 2/1, 3/1 and 4/1 Zn/Cr atomic ratios. Every catalyst sample was then analysed by EPMA. The analysis was performed by integrating the counts for a preset lifetime and for a large number of different positions over the sample at various magnifications, to reduce errors due to possible inhomogeneity of the sample. The Zn/Cr ratios obtained from these measurements were averaged for each sample and compared with calibration graphs obtained similarly with the standards. The measurements were repeated after carefully and finely grinding each sample in the mortar. No difference was noticed between the Zn/Cr values so determined on unground and ground samples, showing a good homogeneity of the samples and the absence on any segregation between bulk and surface. The micrographs taken by SEM in several points at either 200 or 2000 × magnification showed in any case rather small crystals arrayed in high disorder, with no remarkable difference between any samples, either as prepared or reduced. XRD analysis of the reduced samples (Fig. 1)

TABLE I Principal physico-chemical characteristic of the catalysts employed

Catalyst	Zn/Cr atomic ratio	BET surface area ($m^2 g^{-1}$)	Total pore volume ($cm^3 g^{-1}$)	Average pore radius (nm)
A	2.7	57.5	0.5	4.5
B	3.0	60.8	1.0	3.5
C	3.4	63.3	2.6	3.5 and 15.0[a]

[a] 14 and 86% of total pore volume, respectively.

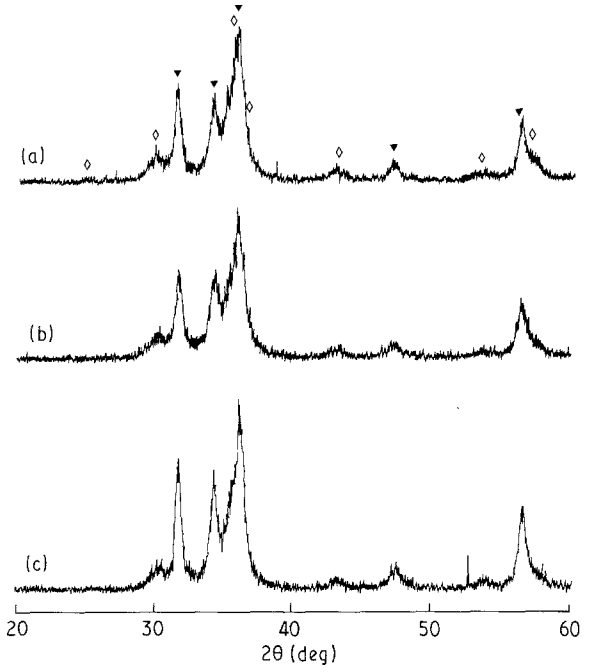

Figure 1 *X*-Ray diffractogram obtained with the reduced catalyst. JCPDS file No. [10]: (▼) ZnO, zincite 5-0664; (◇) $ZnCr_2O_4$, 22–1107. (a), (b) and (c) are for reduced A, B and C samples, respectively.

also failed to reveal any noteworthy difference with respect to unreduced ones. Only ZnO and $ZnCr_2O_4$ phases [10] were ever detected, with absence of any further diffraction line.

A comparison was made between the present results for surface area, porosity, XRD and SEM analysis and those given [1] by finished catalysts of similar composition (Zn/Cr = 3), but prepared by coprecipitation or through the wet-mixing procedure. It should be noticed that, since the optimal reaction temperature for the catalytic synthesis of MP was found to be about 400 °C [2], all the catalysts were calcined up to 440 °C, in order to confer thermal stability to the solid under the reaction conditions. The comparison showed that coprecipitation leads to less crystalline solids, possessing also the highest surface area (ca. 75 $m^2 g^{-1}$) and porosity. The wet-mixing procedure leads to the highest crystallinity, accompanied by the lowest surface area (less than 20 $m^2 g^{-1}$) and porosity. The sol–gel technique leads to a catalyst of high surface area (Table I), only slightly lower than that shown by the coprecipitated samples. However, the solid also possesses a rather high degree of crystallinity, similar to that provided by the wet-mixing technique. These findings were confirmed by SEM analysis, showing microcrystals 0.5 to 1 μm in size for samples prepared either by the wet-mixing or by the sol–gel technique, and microcrystals even one order of magnitude smaller for the samples prepared by coprecipitation.

3.3. TPD–TPR tests

3.3.1. Preadsorption of PG followed by TPD ramp

This series of runs showed the nature of the byproducts coming from the diol only, at relatively low temperatures. A typical example of mass spectra monitored during the TPD ramp is shown in Fig. 2. The formation of ethanol, propanol, acetone and methylethyl ketone (MEK) was confirmed, together with the high affinity of PG for the catalyst [4]. Indeed, the shape of the a.m.u. = 46 spectrum in Fig. 2 shows that very probably this reactant adsorbs on to several types of site. From lower-energy sites it desorbs unaltered at low temperature (ca. 280 °C); on the other sites it can be activated for the reaction, so that only a part of it can be desorbed unaltered (higher-temperature desorption peaks), the remaining part being converted into the various products.

3.3.2. Pulses of pure PG under isothermal conditions

This series of 390 °C runs confirmed the high reactivity of PG. The formation of water, carbon dioxide, acetone, acrolein, MEK, propene, ethanol and propanol (a.m.u. characteristic values = 18, 44, 58, 56, 72, 42, 46 and 57, respectively) [4, 5] was observed in respect of every pulse of PG. A typical example of some of the spectra monitored during these runs is given in Fig. 3.

3.3.3. Preadsorption of ED followed by TPD ramp and pulses of pure ED under isothermal conditions

The TPD ramps carried out after preadsorption of ED (Fig. 4), besides desorption of ED, showed neat peaks of pyrazine but no traces of the a.m.u. = 84 fragment

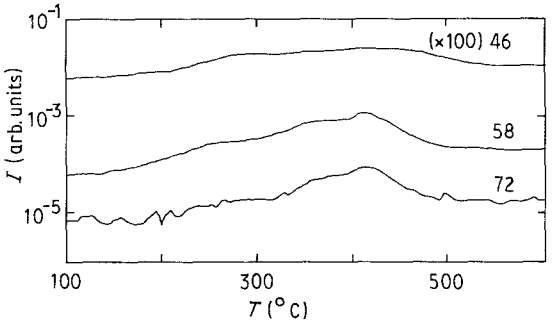

Figure 2 Typical example of some of the mass spectra monitored during the TPD ramp (20 K min^{-1}) following preadsorption of PG at 100 °C on catalyst A: desorption of acetone (a.m.u = 58), MEK (72) and PG (46).

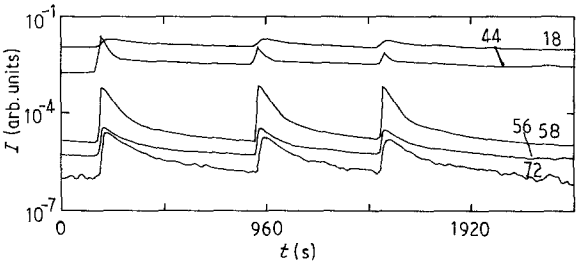

Figure 3 Typical example of mass spectra monitored during an isothermal run (390 °C) with three pulses of pure PG. (catalyst A). A.m.u. values: 18, water; 44, CO_2; 58, acetone; 56, acrolein; 72, MEK.

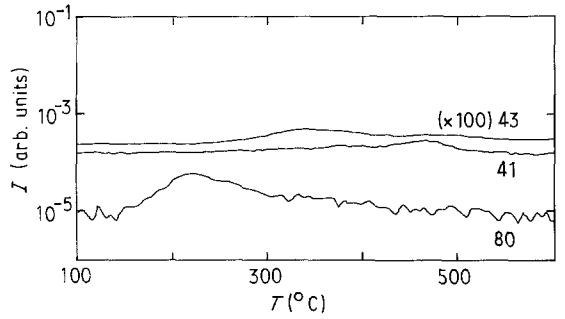

Figure 4 Typical example of mass spectra monitored during the TPD ramp (20 K min^{-1}) following preadsorption of ED at 100 °C (catalyst A). A.m.u. values: 41, hydrogenated pyrazinic species; 43, ED; 80, pyrazine.

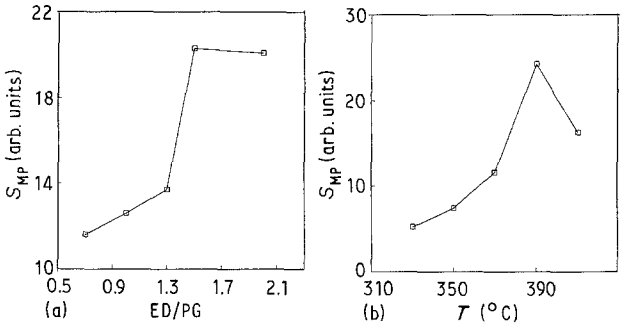

Figure 6 Trend of MP peak area as a function of (a) ED/PG feeding molar ratio (reaction temperature 390 °C) and (b) reaction temperature (ED/PG = 1/1). All other reaction parameters kept constant.

typical of tetrahydropyrazine (THP), a kinetic intermediate detected in previous work [4, 5]. Nevertheless, the formation of some hydrogenated pyrazines must be admitted, since the signal for a.m.u. = 41, a typical fragment of these species, was always more intense than that for a.m.u. = 43, in spite of the fact that the latter is more intense in the fragmentation spectrum of pure ED. A low-intensity 41 fragment is also present in the pattern of pyrazine. However, the trend of 41, unparallel to the a.m.u. = 80 fragment (see Fig. 4), clearly indicates a different source with respect to the fragmentation of pyrazine. All these findings were confirmed by the runs carried out by injecting pulses of pure ED under isothermal conditions (390 °C).

3.3.4. Isothermal runs with pulses of ED + PG mixture

The pulse injections of ED + PG mixture under isothermal conditions (Fig. 5) showed in any case the formation of the main reaction product MP, together with pyrazine, acetone and lower amounts of MEK and propionitrile. The optimal reaction conditions in these pulse-reactor experiments were determined by plotting the area under the peak characteristic of the main product (MP) as a function of the ED/PG feeding ratio at constant temperature (390 °C) or as a function of reaction temperature at constant ED/PG molar ratio (1/1), the remaining reaction parameters being rigorously constant. Fig. 6 shows that such values are ED/PG = 1.5 and T = 390 °C, respectively. The latter confirms the value found for both coprecipitated and wet-mixed catalyst [2, 4].

3.3.5. TPD runs after preadsorption of ED + PG

After preadsorption of ED + PG through the injection of an equimolar mixture of the two reactants during the initial 100 °C isotherm, the following TPD ramp (Fig. 7) showed the desorption of unconverted reactants, of the desired product (MP) and of the main byproducts (acetone and pyrazine). It may be noted (see Fig. 7) that all the products, especially pyrazine, desorb at lower temperatures with respect to the reactants, which show a much higher affinity for the catalyst. Some runs carried out after separated preadsorption of ED before PG or of PG before ED showed that a larger amount of MP forms when PG is preadsorbed before ED, than vice versa (peak area = 7.75 of 4.95, respectively, as measured in the same arbitrary units).

3.3.6. Pulses of one reactant during the desorption of the other

This series of runs aimed at detecting the reaction intermediates helpful for the determination of the reaction mechanism. It was noticed that pulses of PG, injected during the TPD ramp following the preadsorption of such a reactant, gave the formation of tiny peaks of dihydromethylpyrazine (DHMP, a.m.u. = 96), tetrahydro-methylpyrazine (THMP, 98) and

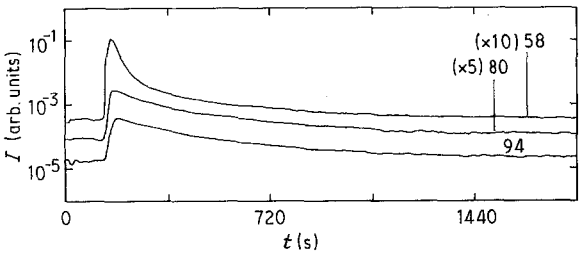

Figure 5 Typical example of mass spectra monitored during an isothermal run (390 °C), with only one pulse of ED + PG mixture (catalyst A). ED/PG feeding molar ratio = 1. A.m.u. values: 58, acetone; 80, pyrazine; 94, MP.

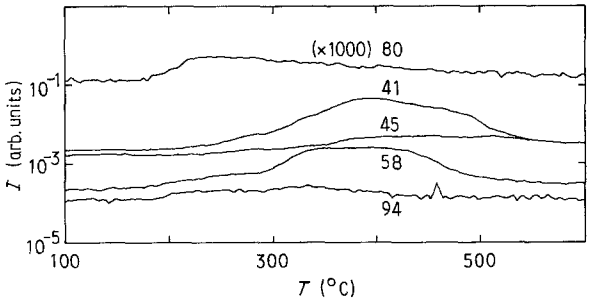

Figure 7 Typical example of mass spectra monitored during the TPD ramp (20 K min^{-1}) following preadsorption of an equimolar mixture of ED + PG (catalyst A). A.m.u. values: 41, ED; 45, PG; 58, acetone; 80, Pyrazine; 94, MP.

methylpiperazine (MPIP, 100 and 85). On the other hand, no trace of such intermediates was ever noticed by injecting pulses of ED during the desorption of PG. These findings, coupled with the larger amount of MP forming under the latter conditions, confirm not only the reaction path proposed [4, 5] for the coprecipitated catalyst, namely initial formation of the fully hydrogenated MPIP followed by progressive and rapid dehydrogenation down to MP, but also that in the latter case the reaction proceeds more rapidly than in the former, so that the reaction intermediates can no more be detected [4].

By plotting the selectivity to the desired product, as measured from the area of the desorption peak of MP under identical conditions (Fig 8), it may be seen that the maximum is attained for catalyst B, i.e. for the catalyst in which the Zn/Cr atomic ratio is 3/1. This confirms the dependence of selectivity on Zn/Cr ratio shown by the catalysts prepared both by coprecipitation and by the wet-mixing procedure [1, 2, 4], so showing the importance of the Zn/Cr ratio as a fundamental parameter for governing the behaviour of the catalyst.

3.4. EPR analysis

All the samples gave an EPR pattern (Fig. 9) composed of a strong symmetric Lorentzian-shaped line centred at $g = 1.98$ and of a much weaker line centred at ca. g = 4. The latter is due to $\Delta M_s = 2$ "forbidden" transition and it is characteristic of triplet state formation in powder samples [11]. The former is characteristic [12–14] of Cr^{3+} ions so closely clustered together that the strong spin–spin exchange partially "washes out" the line-broadening effect due to the spin–spin dipolar interaction, yielding a Lorentzian-shaped narrowed line (bulk-, or β-Cr^{3+}). Fig. 10 shows an example of best fitting [15] of the Lorentzian-shaped model (full line) to the more intense line of an experimental spectrum. The line-width was also strongly temperature-dependent, as reported in the literature for similar compounds [12–14], in agreement with the theory of Huber [16] and Maleev [17] for antiferromagnetic systems above their Néel temperature. However, the range of this variation is typical of each species. The β-Cr^{3+} EPR line-width is reported to vary from about 2000 to 800 G with chromia–alumina reduced in hydrogen at 773 K [12], while with antiferromagnetic $ZnCr_2O_4$, having a normal spinel structure, at the same temperature it was found to be less than 300 G broad. With ZnO–$ZnCr_2O_4$ solid mixtures to which a small amount of Pd (0.73 wt %) was added, we found it to range from 360 to 250 G [14]. The present case appears as intermediate among the above-mentioned ones, the EPR line-width ranging between 650 and 390 G (Fig. 11).

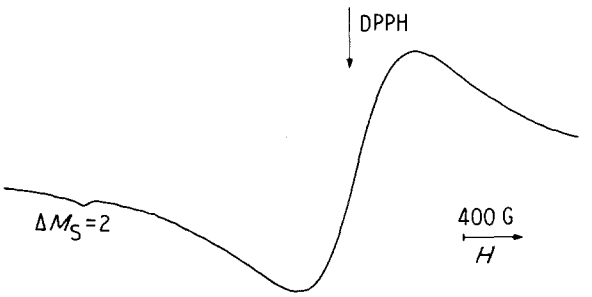

Figure 9 EPR pattern recorded with catalyst A at room temperature. The weak line at ca. $g = 4$ (left-hand side of spectrum) is typically due to a $\Delta M_s = 2$ "forbidden" transition, characteristic of triplet state formation in oxide powders.

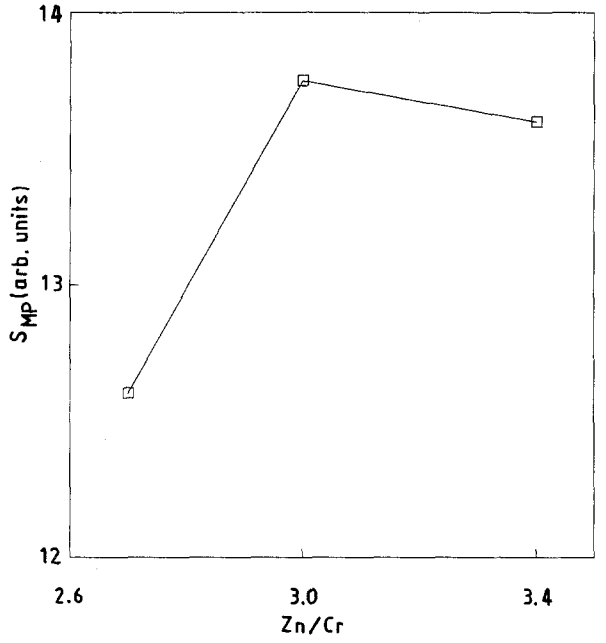

Figure 8 Dependence on the Zn/Cr ratio of selectivity to the desired product (MP), as calculated from a.m.u. = 94 peak area in pulse-reactor runs at 390 °C under identical experimental conditions.

In any case a great influence on the EPR spectral shape is always exerted by even small variations in the geometry of the compound. Indeed, the two competitive effects of spin–spin dipolar broadening and spin–spin exchange narrowing are acting at the same time on the paramagnetic systems, with different dependence on metal–metal distance, the former acting at longer distances than the latter. When the spin–spin exchange is strong enough, a nearly Lorentzian-shaped EPR line results, the width of which is given by [18]

$$\delta H \propto H_p^2 / H_e$$

where H_p^2 is the mean square magnetic field produced by the dipolar interaction between the electron spin and H_e is the field produced by exchange interaction between them. For instance, it has been reported [19] that it suffices to substitute S with Se in $AgCrS_2$ to have a completely different (ferromagnetic) behaviour, and small additions of Pd as well as variations of Zn/Cr ratio strongly affect the EPR line-width of coprecipitated ZnO–$ZnCr_2O_4$ solid mixtures [14]. The last effect is also observed in the present case, as shown in Fig. 11: a slightly larger EPR line-width is noticed at any temperature when Zn/Cr = 3 (catalyst B). Both for lower (2.6) and higher (3.4) Zn/Cr ratio (catalysts A and C, respectively) a slightly narrower

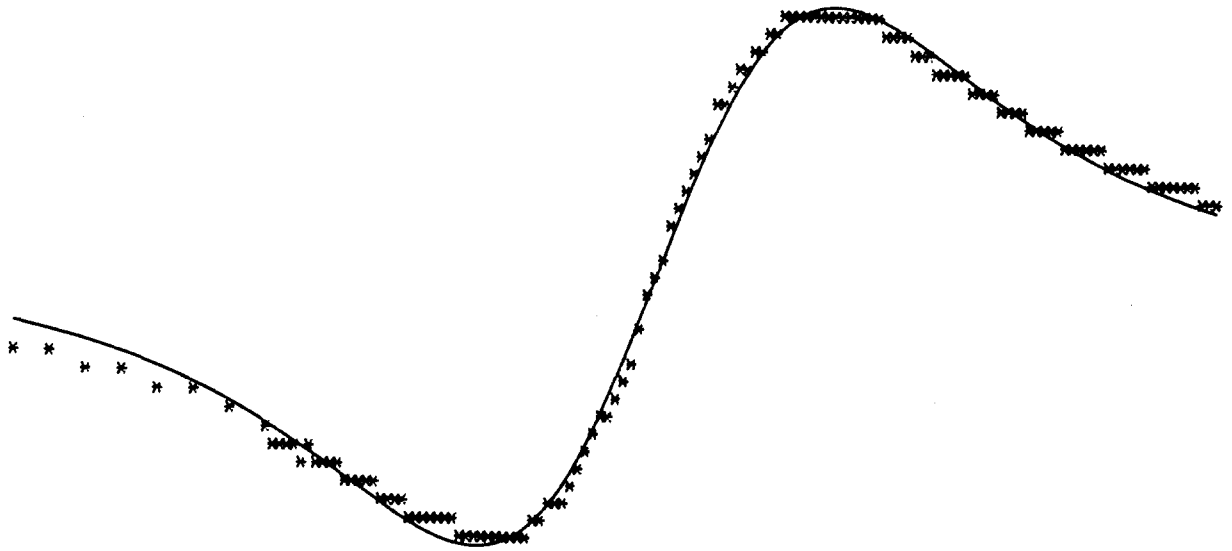

Figure 10 Example of best fitting of the Lorentzian-shaped model (full line) to the strong line of an experimental spectrum.

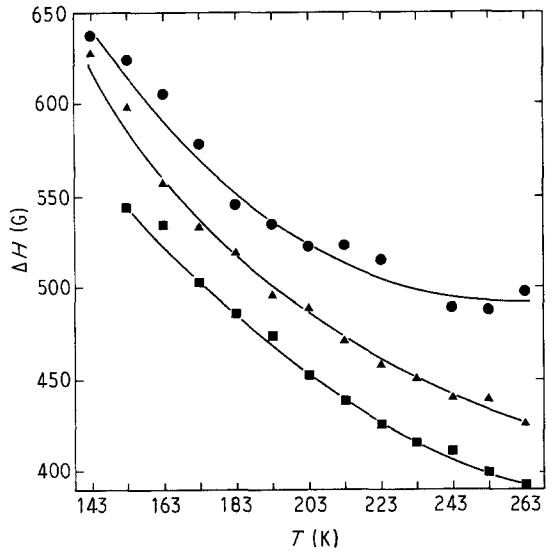

Figure 11 Dependence on temperature of the width of the Lorentzian-shaped line of the EPR spectra of catalysts (■) A, (●) B and (▲) C (see Table I).

EPR line is detected. An analogous behaviour was reported [14] for coprecipitated $ZnO–ZnCr_2O_4$, promoted with 1 wt % Pd, for which the EPR line-width broadened for Zn/Cr $\simeq 3$. This was interpreted as being due to the fact that the exchange line-narrowing acts at shorter distances than dipolar line-broadening. Indeed, it is known [20–22] that an increase in the Zn/Cr ratio is accompanied by an increase in the crystal lattice parameters of the spinel phase ($ZnCr_2O_4$) present in this solid, from 0.836 nm (Zn/Cr = 0.5) up to 0.841 nm (Zn/Cr = 3), followed by a decrease down to 0.839 nm with a further increase in the ratio to Zn/Cr = 5.7. A maximum of the lattice parameters and consequently of the average metal–metal distance is thus attained for Zn/Cr = 3, resulting in a less effective spin–spin exchange narrowing effect with respect to that generated by shorter metal–metal distance. Hence, a broader EPR line is generated.

4. Conclusions

The conclusions one may draw from the present study can be summarized as follows.

1. The structure of the oxide mixture depends rather strongly on the method of preparation.
2. The wet-mixing procedure leads to the highest degree of crystallinity, characterized by the lowest surface area and porosity, while coprecipitation gives opposite results. The sol–gel technique leads to a mixture of intermediate characteristics, with the surface area and porosity only slightly lower, but the crystal size considerably larger than for coprecipitation.
3. The catalytic behaviour of the solid obtained depends strongly not only on the Zn/Cr ratio, but also on the method of preparation, the highest selectivity corresponding to Zn/Cr = 3 and to lower crystal size, leading to the highest surface area and porosity.
4. The resulting line-width of the EPR signal, generated by the Cr^{3+} ions of the solid and due to the opposite effects of two counteracting phenomena, may constitute a useful probe for monitoring both the intimate structure and catalytic behaviour of the material.

References

1. L. FORNI, *J. Catal.* **111** (1988) 199.
2. L. FORNI and S. NESTORI, in "Heterogeneous Catalysis and Fine Chemicals", edited by M. Guisnet, J. Barrault, C. Bouchoule, D. Duprez, C. Montassier and G. Pérot, Studies in Surface Science and Catalysis Vol. 41 (Elsevier, Amsterdam, 1988) p. 291.
3. L. FORNI and C. OLIVA, *J. Chem. Soc. Faraday Trans. I* **84** (1988) 2477.
4. L. FORNI and P. POLLESEL, *J. Catal.* **130** (1991) 403.
5. L. FORNI and R. MIGLIO, in "Heterogeneous Catalysis and Fine Chemicals II", edited by M. Guisnet, J. Barrault, C. Bouchoule, D. Duprez, G. Pérot, R. Maurel and C. Montassier, Studies in Surface Science and Catalysis Vol. 59 (Elsevier, Amsterdam, 1991) p. 367.
6. L. FORNI, M. TOSCANO and P. POLLESEL, *J. Catal.* **130** (1991) 392.

7. S. R. HELLER and G. W. A. MILNE, "EPA-NIH Mass Spectral Data Base", Vols 1 and 5 (US Government Printing Office/National Bureau of Standards, Washington, DC, 1978).
8. R. D. CRAIG and E. H. HARDEN, *Vacuum* **16** (1966) 67.
9. C. N. SATTERFIELD, "Heterogeneous Catalysis in Practice" (McGraw-Hill, New York, 1980) p. 123.
10. "Selected Powder Diffraction Data, Miner. DBM" (Vol. 1–23) (JCPDS, Swarthmore, Pennsylvania, 1974).
11. J. E. WERTZ and J. B. BOLTON, "Electron Spin Resonance" (McGraw-Hill, New York, 1972) p. 242.
12. D. E. O'REILLY and D. S. MACIVER, *J. Phys. Chem.* **66** (1962) 276.
13. M. BARAN, S. PIECHOTA and A. PAJACZKOWSKA, *Acta Phys. Polonica* **A59** (1981) 47.
14. L. FORNI and C. OLIVA, *J. Chem. Soc. Faraday Trans. 1* **84** (1988) 2477.
15. M. BARZAGHI and M. SIMONETTA, *J. Magn. Reson.* **54** (1983) 216.
16. D. L. HUBER, *J. Phys. Chem. Solids* **32** (1971) 2145.
17. S. V. MALEEV, *Phys. Lett.* **A47** (1974) 111.
18. P. W. ANDERSON and P. R. WEISS, *Rev. Mod. Phys.* **25** (1953) 869.
19. R. E. BENFIELD, P. P. EDWARDS and A. M. STACY, *J. Chem. Soc. Faraday Trans. 1* **83** (1987) 3527.
20. M. BERTOLDI, G. BUSCA, B. FUBINI, E. GIAMELLO and A. VACCARI, in Proceedings of 6th Italian-Czechoslovak Symposium on Catalysis, San Remo, September 1987 (Societa' Chimica Italiana) p. 156
21. M. BERTOLDI, G. BUSCA, B. FUBINI, E. GIAMELLO, F. TRIFIRO' and A. VACCARI, *J. Chem. Soc. Faraday Trans. 1* **84** (1989) 237.
22. G. DEL PIERO, M. DI CONCA, F. TRIFIRO' and A. VACCARI, in "Reactivity of Solids", edited by P. Barret and L. C. Dufour, (Elsevier, Amsterdam, 1985) p. 1029.

Received 8 May
and accepted 17 November 1992